COMPARING THE THREE POSSIBLE SCALINGS OF STREAM-WISE NORMAL STRESS IN TURBULENT BOUNDARY LAYERS

Peter A. Monkewitz
Faculty of Engr. Science
Swiss Federal Inst. Technology
CH-1015 Lausanne, Switzerland
peter.monkewitz@epfl.ch

Hassan M. Nagib
MMAE Department
Illinois Inst. Technology
Chicago, IL 60616, USA
nagib@iit.edu

Vincent Boulanger
MMAE Department
Illinois Inst. Technology
Chicago, IL 60616, USA
vncnt.bou@gmail.com

ABSTRACT

The focus of this contribution is an evaluation against experimental data of three models for the stream-wise normal stress in zero pressure gradient turbulent boundary layers, henceforth abbreviated ZPG TBL's : an inner-scaled, mixed-scaled and outer-scaled model, where the stress is scaled by the square of the friction velocity, the product of friction and free stream velocities, and the square of the free stream velocity, respectively. The inner-scaled model of Monkewitz & Nagib (2015), which implies a decrease of the (negative) outer logarithmic slope of the stream-wise normal stress with increasing Reynolds number and is the only model constructed as a genuine composite asymptotic expansion satisfying the complete momentum equation close to the wall, is found to provide the closest fit to the experimental data. As an aside, it is shown that these data do not collapse in the so-called diagnostic plot.

I. INTRODUCTION

The central theme of this paper is the Reynolds number scaling of the stream-wise normal stress $\langle uu\rangle$, in particulat of its inner maximum, of the height of the outer plateau or outer peak and of the start of its presumed logarithmic decrease towards the outer boundary layer edge. To unify the discussion, $\langle uu\rangle^+$ will be specified throughout this paper in inner units, i.e. normalized by the square of the friction velocity $u_\tau^2 \equiv (\tau_{\rm wall}/\rho)$.

The paper first recalls in section II the connection between the scaling of the outer plateau or peak, its location and the (outer) logarithmic slope of $\langle uu\rangle^+$, in particular the necessary conditions for the latter to be independent of Reynolds number. The inner-scaled, mixed-scaled and outer scaled models considered here are introduced in section III and compared to experimental data in section IV. In its last sub-section IV.3, the important question is investigated of what Reynolds number is required to reliably determine the logarithmic slope of $\langle uu\rangle^+$. Using the same data and the inner-scaled model, it is demonstrated in the appendix that the "diagnostic plot" of $u_{mathrmrms}/U$ versus U/U_∞ introduced by Alfredsson *et al.* (2011) collapses the data only over a limited low Reynolds number range. The paper closes with brief conclusions in favor of the inner-scaled model in section V.

II. THE CONNECTION BETWEEN LOGARITHMIC SLOPE AND SCALING OF STREAM-WISE NORMAL STRESS

According to the current "majority view" (see e.g. Marusic *et al.* (2013)), the stream-wise normal stress decays logarithmically between the outer plateau or outer peak "outp" and a wall-normal station near the boundary layer edge. The purpose of this section is to determine the relation between the range of the supposed logarithmic decay and the magnitude of the stream-wise normal stress $\langle uu\rangle$ at the start of the logarithmic decay.

For the purpose of the following discussion, the scaling $\sigma_{\rm uu}({\rm Re}_\tau)$ of the normal stress is specified explicitly, such that

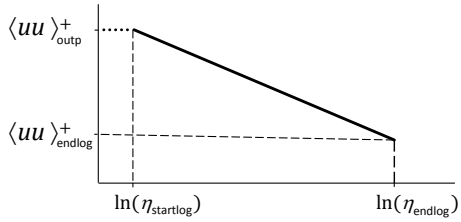

Figure 1. Schematic of the logarithmic region of $\langle uu\rangle^+$, with $\eta \equiv y/\delta$ the outer wall-normal coordinate.

$\langle uu\rangle \equiv \sigma_{\rm uu}\langle uu\rangle^+ = \mathcal{O}(1)$, where ${\rm Re}_\tau$ is the Reynolds number based on boundary layer thickness δ and u_τ. In the wall-normal direction, the logarithmic decay region is taken to extend from $\eta_{\rm startlog}$ to $\eta_{\rm endlog}$, where $\eta \equiv (y/\delta) = (y^+/{\rm Re}_\tau)$ with $y^+ \equiv (yu_\tau)/\nu$ the standard inner-scaled coordinate. The conversion from η to the outer Rotta-Clauser coordinate $Y \equiv (yu_\tau)/(U_\infty\delta_*) \equiv \eta({\rm Re}_\tau/{\rm Re}_{\delta_*})$ involves the conversion from ${\rm Re}_\tau$ to ${\rm Re}_{\delta_*}$, the Reynolds number based on displacement thickness δ_* and free stream velocity U_∞. As the definition of the boundary layer thickness δ is somewhat arbitrary and varies from author to author, the conversion adopted in this paper will be specified in section IV.

The logarithmic decay region of $\langle uu\rangle^+$ is shown schematically in figure 1. To obtain the scaling of the logarithmic slope, the starting point of the logarithmic decay is taken to scale as $\sigma_{\rm startlog}({\rm Re}_{\delta_*})\eta_{\rm startlog} = \mathcal{O}(1)$, while $\eta_{\rm endlog} \approx 1$. Together with $\langle uu\rangle^+(\eta_{\rm startlog}) \gg \langle uu\rangle^+(\eta_{\rm endlog})$, one obtains for the logarithmic slope LS of $\langle uu\rangle^+$

$$LS = \mathcal{O}\left(\frac{-1}{\sigma_{\rm uu}\ln(\sigma_{\rm startlog})}\right) \qquad (1)$$

Therefore, for any power-law scaling $\sigma_{\rm startlog} = {\rm Re}_\tau^\alpha$, a constant logarithmic slope of $\langle uu\rangle^+$ is only possible for $\sigma_{\rm uu} = \mathcal{O}(\ln{\rm Re}_\tau)^{-1} \sim (U_\infty^+)^{-1}$, i.e. for a "mixed" scaling of $\langle uu\rangle_{\rm outp}$. Specifically, to obtain a universal (Reynolds independent) logarithmic decay rate (the "Townsend-Perry constant") beyond $\eta \approx 3{\rm Re}_\tau^{-1/2}$, as suggested by Marusic *et al.* (2013), $\langle uu\rangle^+_{\rm outp}$ would **have** to be $\mathcal{O}(\ln{\rm Re}_\tau) \sim \mathcal{O}(U_\infty^+)$. Since Monkewitz & Nagib (2015) have demonstrated that near the wall the inner scaling, i.e. $\langle uu\rangle^+ = \mathcal{O}(1)$, is the only one compatible with the momentum equation, this would imply a boost of $\langle uu\rangle^+$ by a factor of order $\mathcal{O}(\ln{\rm Re}_\tau)$ between the near-wall region and the start of the logarithmic decay. To date, no mechanism to achieve this has been proposed.

III. MODELS OF NORMAL STRESS, REPRESENTATIVE OF THE THREE MAIN SCALING OPTIONS

In the following, we consider three models representative of the three main options for scaling streamwise normal stress:

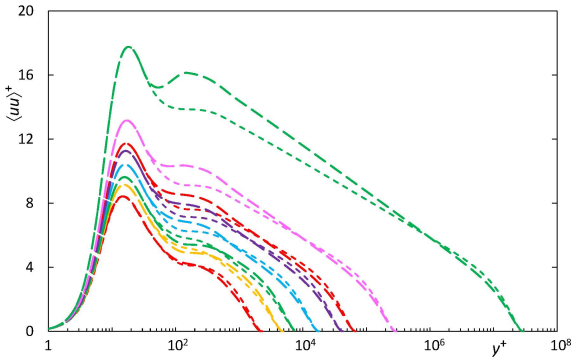

Figure 2. Comparison of the "attached eddy" models with logarithmic slopes of -1.03 (short dashes) and -1.26 (long dashes) for the Reynolds numbers of table 1

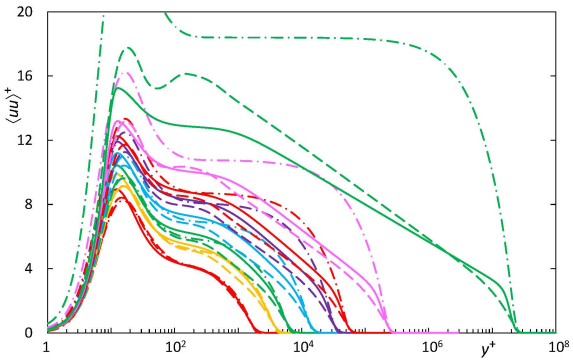

Figure 3. Comparison between the inner model of Monkewitz & Nagib (2015) (solid lines), the attached eddy model with a logarithmic slope of -1.26 (dashed lines) and the outer model of Duncan (2011) (dash-dotted lines) for the Reynolds numbers of table 1

- Inner scaling - $\langle uu\rangle = \mathscr{O}(u_\tau^2)$, i.e. $\langle uu\rangle^+ = \mathscr{O}(1)$
- Mixed scaling - $\langle uu\rangle = \mathscr{O}(U_\infty u_\tau)$, i.e. $\langle uu\rangle^+ = \mathscr{O}(U_\infty^+)$
- Outer scaling - $\langle uu\rangle = \mathscr{O}(U_\infty^2)$, i.e. $\langle uu\rangle^+ = \mathscr{O}(U_\infty^+)^2$

The **inner-scaled model** considered here has been proposed by Monkewitz & Nagib (2015) and is the only one of the three models constructed in terms of matched inner and outer asymptotic expansions. They showed by a detailed analysis of the complete Taylor-expanded momentum equations that close to the wall (up to y^+ of around 10) $\langle uu\rangle^+$ must be $\mathscr{O}(1)$. Keeping the inner scaling throughout the boundary layer, the observed increase of the inner peak at $y^+ \approx 15$ is modelled as $\langle uu\rangle^+_{\text{i.peak}} \cong 22 - 340/U_\infty^+$, in excellent agreement with all available data. The outer expansion features a logarithmic decay, starting at $y^+ = \mathscr{O}(U_\infty^+)$ with a Reynolds number dependent slope of $-52/U_\infty^+$. The inner and outer expansions are asymptotically matched through an "outer plateau" of height $22 - 470/U_\infty^+$, centered at $y^+ = \mathscr{O}(U_\infty^+)^{1/2}$.

The **mixed model** has been inspired by the attached eddy hypothesis of Townsend (1956, 1972) and first developed for the wake part by Marusic & Perry (1995) and Marusic *et al.* (1997). The main characteristic of this model, which follows from the attached eddy hypothesis, is a Reynolds-independent logarithmic slope of $\langle uu\rangle^+$ in the outer part of the boundary layer. As a consequence, $\langle uu\rangle^+(\eta_{\text{outp}}$ in figure 1 is of order U_∞^+ as discussed in section II. Marusic & Kunkel (2003) then completed the model by patching a near-wall fit to the outer part which had a logarithmic slope of -1.03. Finally, Marusic *et al.* (2013) changed the logarithmic slope to -1.26 to adapt the model to more recent data. The modified patch to the near-wall fit of Marusic & Kunkel (2003) was provided by Marusic (2016). The models with the original "Townsend-Perry constant" of -1.03 and the modified value of -1.26 are shown in figure 2 for the Reynolds numbers of table 1.

Finally, the **outer model** of Duncan (2011) is considered. Its main difference to the inner model of Monkewitz & Nagib (2015) and the attached eddy model is the lack of a logarithmic decay in the outer part of the boundary layer. Instead, this fit develops an extended plateau in the wake region at a level of $0.007\,(U_\infty^+)^2$ before a sharp drop to zero at the edge of the boundary layer.

All three models are compared in figure 3 for the Reynolds numbers of table 1.

IV. COMPARISON BETWEEN MODELS AND DATA

IV.1 Choice of experimental data

To ensure consistency, all the Reynolds numbers for the experiments used in this paper and listed in table 1 are derived from U_∞^+:

First Re_{δ_*} is obtained from the relation (Monkewitz (2017))

$$U_\infty^+ = \frac{1}{0.384}\ln(\text{Re}_{\delta_*}) + 3.26 \quad , \tag{2}$$

where the additive constant has been slightly reduced relative to Monkewitz *et al.* (2007). Then, Re_τ based on $\delta_{.995}$ is determined from the graph of $\eta_{.995}$ versus Re_{δ_*} (figure 2 of Monkewitz (2017)), which is obtained from a new composite fit of U^+ in (Monkewitz (2017)). Note that $\eta_{.995}$ is in general a decreasing function of Re_{δ_*} which is sensitive to the outer fit of $U^+(\eta)$. For the fit of Monkewitz (2017), $\eta_{.995}$ is equal to 0.245 at $\text{Re}_{\delta_*} = 10^4$ and decreases by 5% to $\text{Re}_{\delta_*} = 10^8$.

Table 1. Data sources and color scheme for all figures.
† : case #7 at $x = 10.56$ m with $U_\infty = 13.36$ m/s;
‡ : case #11 at $x = 10.56$ m with $U_\infty = 20.18$ m/s.

Re_{δ_*}	Re_τ	symbol	source
7600	1880	■ (red)	Bruns (1998)
16500	4070	▲ (yellow)	Kulandaivelu (2011)
27200	6690	♦ (green)	Marusic *et al.* (2013)
61500	15000	● (blue)	Kulandaivelu (2011)
146000	35600	■ (purple)	Winkel *et al.* (2012)†
233000	56600	▲ (red)	Winkel *et al.* (2012)‡
10^6	241000	— (pink)	fits only
10^8	$2.32\,10^7$	— (green)	fits only

It is important to note here that the **original** LCC data are used, as provided in Winkel *et al.* (2012), while in Marusic *et al.* (2013) $\langle uu\rangle^+$ and y^+ have been rescaled with a u_τ determined by fitting a composite expansion to the corresponding U^+. However, all the LCC mean velocity profiles systematically have an additive log-law constant of about 5.2 instead of the standard value around 4.2 (4.22 in the present paper), as seen in figure 4a for one of the profiles. Hence, least-squares fitting a "good" composite expansion to

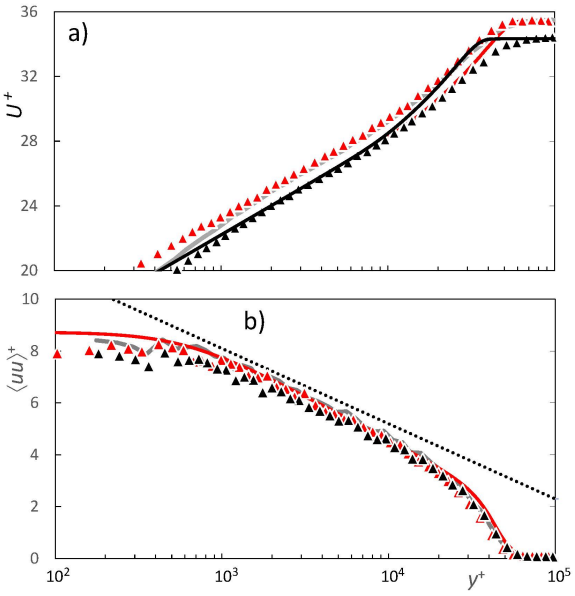

Figure 4. Comparison of the original LCC data for $\mathrm{Re}_{\delta_*} = 2.33\,10^5$ (▲, see table 1) with the rescaled data (▲) of fig. 1 in Marusic *et al.* (2013). a) —, composite fit of Monkewitz (2017) for $\mathrm{Re}_{\delta_*} = 2.33\,10^5$; —, composite fit for $\mathrm{Re}_{\delta_*} = 1.52\,10^5$; — (grey), black triangles back-transformed by a 3% reduction of u_τ. b) Analogous to a) for $\langle uu \rangle^+$, with the outer fit of Monkewitz & Nagib (2015); ···, logarithmic slope of -1.26

the flawed original LCC profile in figure 4a produces an increase of u_τ by approximately 3% which moves the mean velocity profile down and to the right and produces the $U^+(y^+)$ in figure 1 of Marusic *et al.* (2013). However, it is obvious from figure 4a that this approach, which "fixes" the log-law, completely botches the approach to the free stream: while the increase of u_τ reduces U^+_∞ to 34.3, corresponding to $\mathrm{Re}_{\delta_*} = 1.52\,10^5$ (equ. 2), the free stream is only reached at $y^+ \approx 8\,10^4$, which is twice the value at which well-behaved data (and the composite fit) reach the free stream at this Re_{δ_*} (see figure 4a). The conclusion is that the LCC data are NOT afflicted by a systematic error of τ_{wall}, but the reason for the anomaly of U^+ can unfortunately not be reconstructed. Therefore, we will use the original LCC data for $\langle uu \rangle^+$ without the rescaling of Marusic *et al.* (2013). As seen in 4b, this issue is crucial for the determination of logarithmic slopes, which can only be determined with confidence from data beyond about $\mathrm{Re}_{\delta_*} \gtrsim 10^5$, as discussed in section IV.3 (see figure 4b for the effect of the rescaling by Marusic *et al.* (2013) on the logarithmic slope).

IV.2 Experimental data versus the models of Section III

This section is devoted to the comparison between the experimental data of table 1 and the three models introduced in section III: the inner-scaled model of Monkewitz & Nagib (2015) in figure 5, the mixed-scaled attached eddy model of Marusic & Kunkel (2003) with the "Townsend-Perry constant" modified to -1.26 in figure 6, and the outer-scaled model of Duncan (2011) in figure 7.

It is quite obvious from these three figures, that the inner-scaled model of Monkewitz & Nagib (2015) provides the best fit to the data considered here, but, in view of the considerable data uncertainty especially inside of the outer plateau or peak, the attached eddy model cannot be discarded on the basis of this comparison. The reader is nevertheless reminded, that the model of Monkewitz & Nagib (2015) is the only one constructed as a true composite expansion and satisfies the full momentum equation close to the wall. The outer-scaled model of Duncan (2011), on the other hand, is seen in figure 7 to completely miss the decay of $\langle uu \rangle^+$ towards the boundary layer edge, except at the lowest Reynolds numbers.

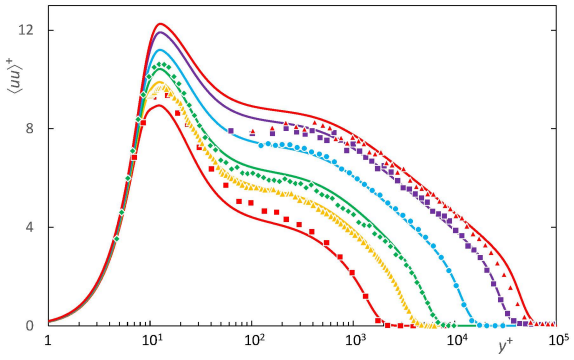

Figure 5. Comparison of $\langle uu \rangle^+$ for the first 6 Reynolds numbers of table 1 with the inner-scaled model of Monkewitz & Nagib (2015).

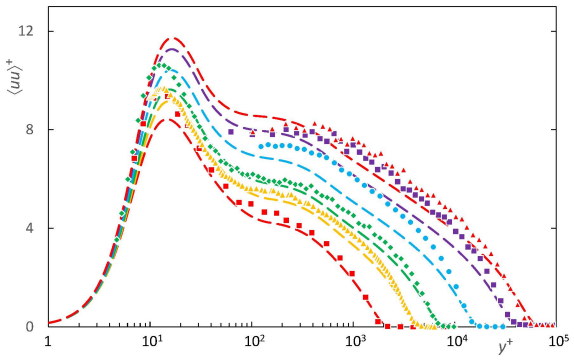

Figure 6. Comparison of $\langle uu \rangle^+$ for the first 6 Reynolds numbers of table 1 with the mixed-scaled model of Marusic & Kunkel (2003) with the modified "Townsend-Perry constant" of -1.26 proposed in Marusic *et al.* (2013).

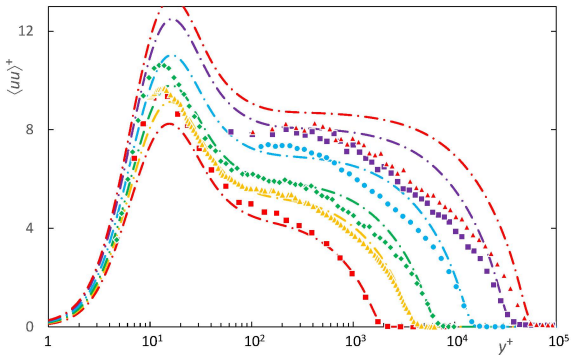

Figure 7. Comparison of $\langle uu \rangle^+$ for the first 6 Reynolds numbers of table 1 with the outer-scaled model of Duncan (2011).

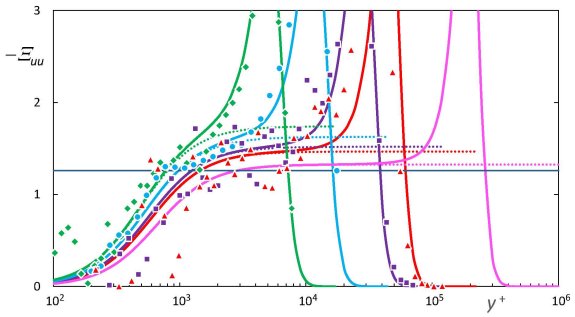

Figure 8. Indicator function Ξ_{uu} (equ. 3) derived from the model of Monkewitz & Nagib (2015) for $27.2\,10^3 \leq \mathrm{Re}_{\delta_*} \leq 10^6$ of table 1. —, complete Ξ_{uu}; $\cdots$, Ξ_{uu} without the final decay towards the boundary layer edge; symbols, Ξ_{uu} derived from corresponding experimental data. Horizontal black line, $\Xi_{uu} = -1.26$. Color scheme and symbols as in table 1.

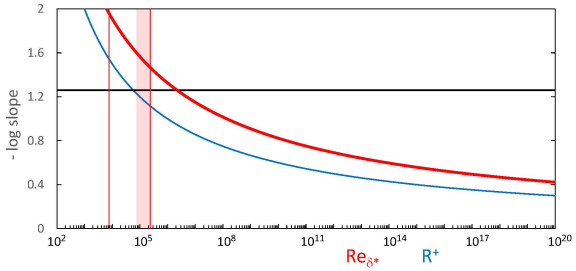

Figure 9. — , underlying logarithmic slope of the outer part of $\langle uu\rangle^+$ versus Re_{δ_*} in the ZPG TBL, according to the inner-scaled model of Monkewitz & Nagib (2015); — , log slope for the pipe versus Re^+ as given in Appendix A of Monkewitz & Nagib (2015). —, -1.26 slope of the attached eddy model. Thin vertical |, range of experimental Re_{δ_*} in table 1. Red-shaded area : range of Re_{δ_*} for which $\langle uu\rangle^+$ starts to have a part with approximately constant logarithmic slope.

IV.3 What Reynolds number is required to reliably determine logarithmic slopes ?

To put the debate about the logarithmic slope of $\langle uu\rangle^+$ in the proper perspective, it is helpful to derive the indicator function

$$\Xi_{uu} = \frac{\mathrm{d}\langle uu\rangle^+}{\mathrm{d}(\ln y^+)} \tag{3}$$

from the experimental data of table 1. This turns out to be considerably more difficult than for the mean velocity, where the logarithmic derivative is commonly used to determine the Kármán constant, since data for $\langle uu\rangle^+$ are much noisier than for U^+. The experimental Ξ_{uu} have been determined with a 5-point quadratic least-squares fit for $\mathrm{Re}_{\delta_*} \geq 16.5\,10^3$ and are shown in figure 8, together with the corresponding indicator functions derived from the model of Monkewitz & Nagib (2015).

Despite the considerable scatter, it is obvious from this figure, that up to $\mathrm{Re}_{\delta_*} \approx 10^5$ it is not possible to determine the underlying logarithmic slope (the horizontal dotted lines in figure 8) by drawing a tangent on the graph of $\langle uu\rangle^+$ versus $\ln(y^+)$. This is because, to use asymptotic matching terminology, the inner and outer parts are not yet sufficiently separated.

Above $\mathrm{Re}_{\delta_*} \approx 10^5$, the experimental points of $-\Xi_{uu}$ in figure 8 are seen to develop, despite the large scatter, a turning point and eventually a plateau at a level which decreases for increasing Re_{δ_*}, but stays above 1.26, the value postulated by the attached eddy model for all Re_{δ_*}. This clearly supports the inner-scaled model of Monkewitz & Nagib (2015). The parameters of its outer fit, however, may well evolve as more high quality data for $\langle uu\rangle^+$ in ZPG TBL's at Reynolds numbers Re_{δ_*} beyond 10^5 become available.

V. CONCLUSIONS IN FAVOR OF INNER-SCALED NORMAL STRESS

The logarithmic slope of $\langle uu\rangle^+$ in the outer part of ZPG TBL's is summarized in figure 9 as a function of Re_{δ_*} for the mixed-scaled attached eddy model of Marusic & Kunkel (2003) and the inner-scaled model of Monkewitz & Nagib (2015). As argued in section IV.3, below Re_{δ_*} of 10^5 this slope cannot be determined directly from the data, but the analysis of the indicator function shows that the turning point of $-\Xi_{uu}$, which eventually develops into the log-region, is a decreasing function of Re_{δ_*} as inferred by Monkewitz & Nagib (2015). The figure 9 also illustrates the difficulty of identifying the dependence of a logarithmic slope on Re_{δ_*} from data over a very narrow range of $\ln(\mathrm{Re}_{\delta_*})$ and the urgent need for high quality data well beyond Re_{δ_*} of 10^5. It is nevertheless noted that the log-slope of the model by Monkewitz & Nagib (2015) crosses -1.26 at $\mathrm{Re}_{\delta_*} \approx 5\,10^6$ which is close to the estimated Reynolds number of the SLTEST atmospheric boundary layer data (see fig. 1 of Marusic *et al.* (2013) and references therein).

Another example, not directly related to the question of the logarithmic slope of $\langle uu\rangle^+$, where an accidental data collapse over the limited range of available experimental Reynolds numbers, is the so-called diagnostic plot, proposed by Alfredsson *et al.* (2011) and briefly discussed in the appendix.

In conclusion, the present paper has once again demonstrated the importance of any model evolving slowly with $\ln(\mathrm{Re}_{\delta_*})$ to incorporate the proper limiting behavior as $\mathrm{Re}_{\delta_*} \to \infty$.

Acknowledgement

We thank Ivan Marusic for graciously providing the code for the attached eddy model and the numerical data of figure 1 in Marusic *et al.* (2013).

APPENDIX: THE "DIAGNOSTIC PLOT"

The so-called diagnostic plot has been proposed by Alfredsson *et al.* (2011) who noticed the collapse of experimental data in the outer part of ZPG TBL's onto a straight line when plotted as u_{rms}/U versus U/U_∞. However, the Reynolds number range was limited and with the availability of the LCC data and the model of Monkewitz & Nagib (2015) for $\langle uu\rangle^+$, it is worthwhile to re-examine this plot. There is however the problem with the mean velocity in the LCC experiment, discussed in section IV.1. Therefore, for the two LCC Reynolds numbers of table 1, only the experimental $\langle uu\rangle^+$ has been retained, while the composite expansion of Monkewitz (2017) has been used for the mean velocity U^+. The diagnostic plot for the Reynolds numbers of table 1 is shown as figure 10 which clearly shows that the supposed collapse onto $u_{\mathrm{rms}}/U = 0.29 - 0.26\,(U/U_\infty)$ is limited to a narrow (low) Reynolds number range.

The additional dotted curves in the figure represent the analogous cross-plot with u_{rms} replaced by the outer asymptotic (pure) logarithmic decay of the Monkewitz & Nagib (2015) model, and U replaced by the mean-flow log-law. As best seen in figure 10b, for $\mathrm{Re}_{\delta_*} \gtrapprox 10^5$ the graphs with U and u_{rms} replaced by their respective log-laws are close to the graphs with the complete composite expansions in the region where the correlation of Alfredsson *et al.*

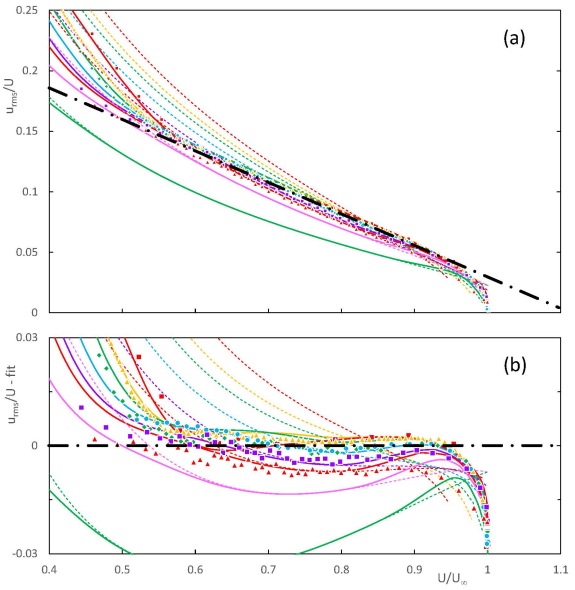

Figure 10. Diagnostic plot according to Alfredsson *et al.* (2011). (a) Data symbols as in table 1; —, corresponding ratios of composite fits for all the data plus $\mathrm{Re}_{\delta_*} = 10^6$ (pink) and 10^9 (green); $\cdots$, corresponding ratios of logarithmic parts; $-\cdot-$, correlation $u_{\mathrm{rms}}/U = 0.29 - 0.26\,(U/U_\infty)$. (b) Same data minus correlation.

(2011) is supposed to hold. Note that the restriction on Re_{δ_*} does not apply with the attached eddy model for $\langle uu\rangle^+$ as, according to Marusic *et al.* (2013), the log regions for U^+ and $\langle uu\rangle^+$ coincide. Hence, the equation $u^+_{\mathrm{rms}}/U^+ = 0.29 - 0.26\,(U^+/U^+_\infty)$ with $U^+ \sim (1/\kappa)\ln(y^+) + B$ and $u^+_{\mathrm{rms}} \sim [c_0 - c_1 \ln(y^+)]^{1/2}$ is clearly unbalanced if the normal stress follows any log-law.

REFERENCES

Alfredsson, P. H., Segalini, A. & Örlü, R. 2011 A new scaling for the streamwise turbulence intensity in wall-bounded turbulent flows and what it tells us about the "outer" peak. *Phys. Fluids* **23**, 041702.

Bruns, Julius M. 1998 Experimental investigation of a three-dimensional turbulent boundary layer in an "S"-shaped duct. PhD thesis, Technische Universität Berlin, Germany.

Duncan, Richard D. 2011 Asymptotic similarity in turbulent boundary layers. PhD thesis, Illinois Institute of Technology.

Kulandaivelu, Vigneshwaran 2011 Evolution and structure of zero pressure gradient turbulent boundary layer. PhD thesis, University of Melbourne.

Marusic, I. 2016 private communication.

Marusic, I. & Kunkel, G. J. 2003 Streamwise turbulence intensity formulation for flat-plate boundary layers. *Phys. Fluids* **15**, 2461–2464.

Marusic, I., Monty, J. P., Hultmark, M. & Smits, A. J. 2013 On the logarithmic region in wall turbulence. *J. Fluid Mech. Rapids* **716**, R3–1–R3–11.

Marusic, I. & Perry, A. E. 1995 A wall wake model for the turbulent structure of boundary layers. Part 2. Further experimental support. *J. Fluid Mech.* **298**, 389–407.

Marusic, I., Uddin, A. K. M. & Perry, A. E. 1997 Similarity law for the streamwise turbulence intensity in zero-pressure-gradient turbulent boundary layers. *Phys. Fluids* **9**, 3718–3726.

Monkewitz, P. A. 2017 Revisiting the quest for a universal log-law and the role of pressure gradient in "canonical" wall-bounded turbulent flows. *subm. to Phys. Rev. Fluids; arXiv 1702.03661* .

Monkewitz, P. A., Chauhan, K. A. & Nagib, H. M. 2007 Self-consistent high-Reynolds-number asymptotics for zero-pressure-gradient turbulent boundary layers. *Phys. Fluids* **19**, 115101.

Monkewitz, P. A. & Nagib, H. M. 2015 Large Reynolds number asymptotics of the stream-wise normal stress in ZPG turbulent boundary layers. *J. Fluid Mech.* **783**, 474–503.

Townsend, A. A. 1956, 1972 *The Structure of Turbulent Shear Flow*. Cambridge University Press.

Winkel, Eric S., Cutbirth, James M., Ceccio, Steven L., Perlin, Marc & Dowling, David R. 2012 Turbulence profiles from a smooth flat-plate turbulent boundary layer at high reynolds number. *Experimental Thermal and Fluid Science* **40**, 140 – 149.